

X. Jin<sup>1</sup>, B. Nergis<sup>2</sup>, A. Rodrigues<sup>2</sup>, S. Bauer<sup>2</sup>, L. Horák<sup>3</sup>, T. Baumbach<sup>2</sup>, V. Holý<sup>3,4</sup>, R. Schneider<sup>1</sup>

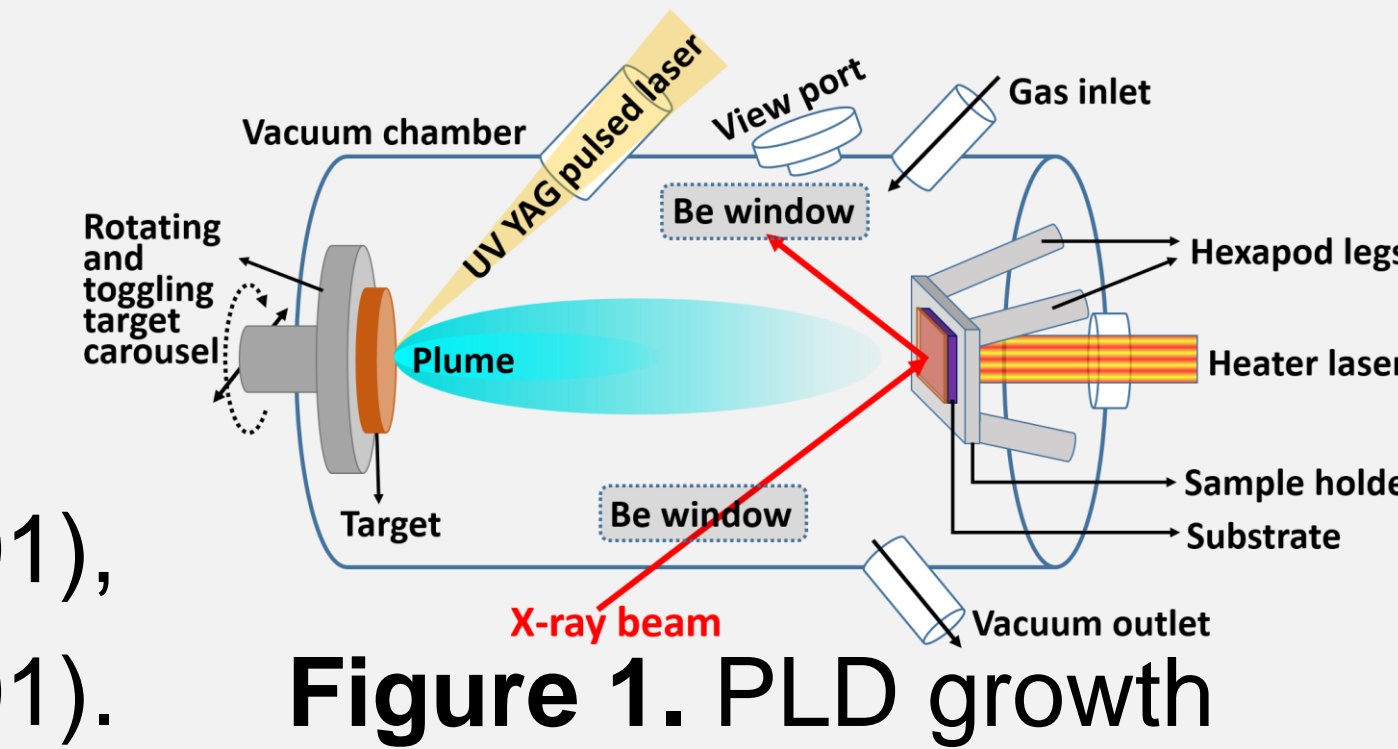
<sup>1</sup>Laboratory for Electron Microscopy, Karlsruhe Institute of Technology (KIT), Engesserstr. 7, D-76131 Karlsruhe, Germany; <sup>2</sup>Institute for Photon Science and Synchrotron Radiation, KIT, Hermann-von-Helmholtz-Platz 1, D-76344 Eggenstein-Leopoldshafen, Germany; <sup>3</sup>Department of Solid State Physics, Charles University, Ke Karlovu 5, 121 16 Prague, Czech Republic; <sup>4</sup>Faculty of Science, Masaryk University, Kotlářská 2, 611 37 Brno, Czech Republic

## Introduction

- Hexagonal ferrites  $h\text{-RFeO}_3$  ( $R = \text{Y, Dy-Lu}$ ), promising candidates for many future applications in information processing and storage [1],
- Epitaxial  $h\text{-LuFeO}_3$  ( $h\text{-LFO}$ ) thin films were deposited on different substrates, e.g.,  $\text{Al}_2\text{O}_3$  (0001),
- Pt interlayer between  $h\text{-LFO}$  and  $\text{Al}_2\text{O}_3$  (0001) to reduce lattice mismatch and to act as a bottom electrode,
- Goal:** Study the thickness effect of the Pt interlayer on the crystalline quality of the  $h\text{-LFO}$  layer.

## LFO thin-film deposition

- Pulsed-laser deposition (PLD) of:
  - $h\text{-LFO}$  (10nm)/ $\text{Al}_2\text{O}_3$  (0001),
  - $h\text{-LFO}$  (10nm)/Pt (20 nm)/ $\text{Al}_2\text{O}_3$  (0001),
  - $h\text{-LFO}$  (10nm)/Pt (40 nm)/ $\text{Al}_2\text{O}_3$  (0001).



## Characterization by electron microscopy

- Topography of the  $h\text{-LFO}$  thin films by secondary-electron (SE) imaging in scanning electron microscopy (SEM), and preparation of cross-sectional TEM lamellae by focused ion beam (FIB) milling, using a Thermo Fisher Dual-beam Helios G4 FX microscope,
- Combined high-angle annular dark-field (HAADF) imaging in scanning transmission electron microscopy (STEM) and energy-dispersive X-ray spectroscopy (EDXS) analyses of the  $h\text{-LFO}/(\text{Pt})/\text{Al}_2\text{O}_3$  interfacial regions at 200 kV with a FEI Tecnai Osiris microscope equipped with a SuperX detector,
- High-resolution transmission electron microscopy (HRTEM) imaging of interfacial regions between  $h\text{-LFO}$  and underlying  $\text{Al}_2\text{O}_3$  substrate or Pt layer.

## SE-imaging results

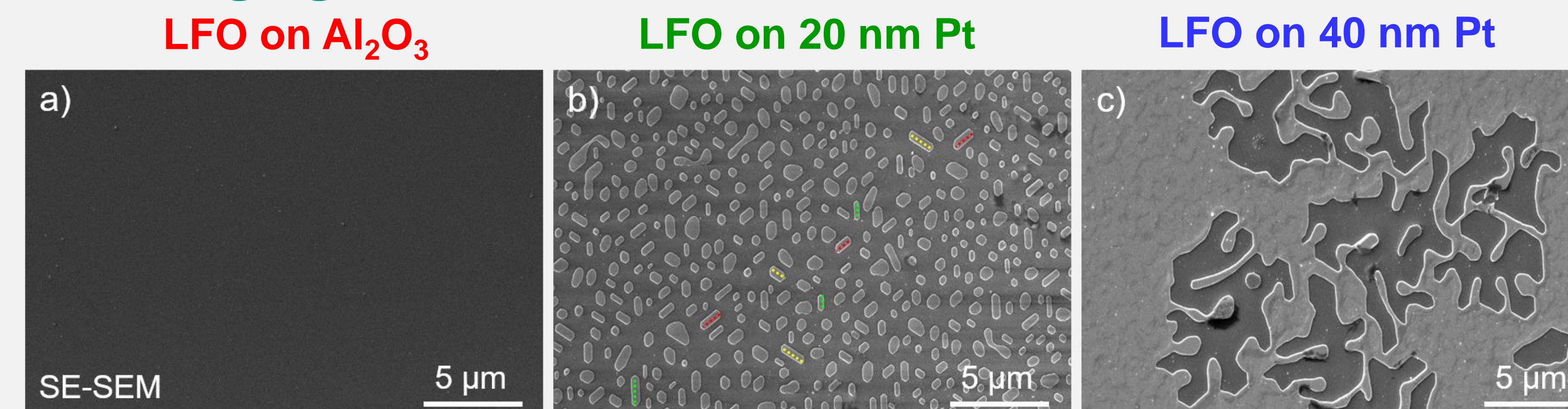


**Figure 2.** Top-view SE-SEM images of the sample surfaces: a) LFO/ $\text{Al}_2\text{O}_3$ , b) LFO/Pt (20 nm)/ $\text{Al}_2\text{O}_3$ , and c) LFO/Pt (40 nm)/ $\text{Al}_2\text{O}_3$ .

- LFO/ $\text{Al}_2\text{O}_3$ : extremely smooth surface,
- LFO/Pt (20 nm)/ $\text{Al}_2\text{O}_3$ : islands with an orientation alignment ( $120^\circ$ ),
- LFO/Pt (40 nm)/ $\text{Al}_2\text{O}_3$ : most of the surface covered by LFO.

## STEM/EDXS results

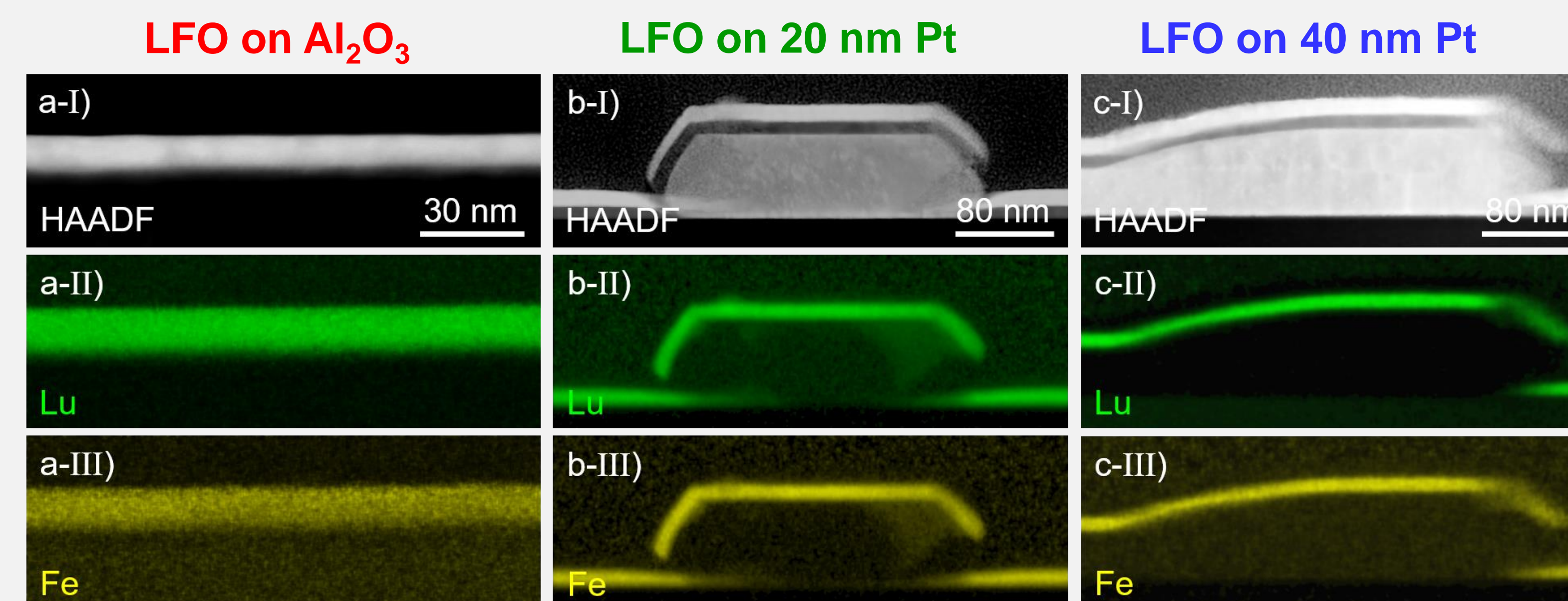


**Figure 3.** Cross-sectional STEM-HAADF images and X-ray maps of the distribution of the elements Lu and Fe for a) LFO/ $\text{Al}_2\text{O}_3$ , b) LFO/Pt (20 nm)/ $\text{Al}_2\text{O}_3$ , and c) LFO/Pt (40 nm)/ $\text{Al}_2\text{O}_3$ .

- LFO/Pt (20 nm)/ $\text{Al}_2\text{O}_3$ : no Pt in island-free regions; LFO layer interrupted by Pt islands,
- LFO/Pt (40 nm)/ $\text{Al}_2\text{O}_3$ : most Pt islands extend to form a Pt layer.

## HRTEM results

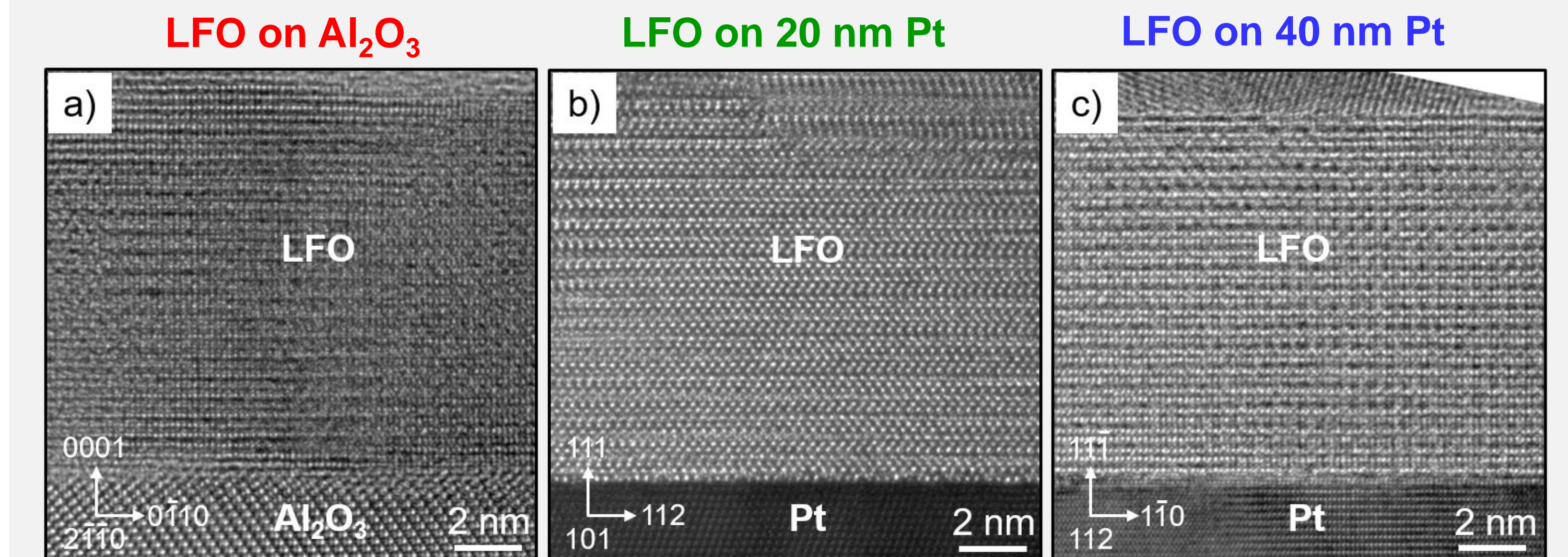


**Figure 4.** Cross-sectional HRTEM images of interfacial regions of a) LFO/ $\text{Al}_2\text{O}_3$ , b) LFO/Pt (20 nm), and c) LFO/Pt (40 nm).

- Hexagonal structure of LFO proved in all three samples,
- LFO/ $\text{Al}_2\text{O}_3$ : low crystalline quality of LFO layer (29 % lattice mismatch) with many crystal defects,
- LFO/Pt (20/40 nm): better crystallinity (mismatch of 6 %) and epitaxial growth.

## Summary

- Crystalline quality of LFO thin films, deposited by PLD on  $\text{Al}_2\text{O}_3$  (0001) or Pt buffered  $\text{Al}_2\text{O}_3$  (0001), improves with increasing thickness of the Pt interlayer.

## References

- H. Schmid, *Ferroelectrics* **162** (1994) 317.
- S. Bauer et al., *Materials* **13** (2020) 61.

The support of Czech Science Foundation (project 19-10799J) and German Research Foundation (projects SCHN 669/11 and BA 1642/8-1) is acknowledged.